



# Nascent HDL (High-Density Lipoprotein) Discs Carry Cholesterol to HDL Spheres

## Effects of HDL Particle Remodeling on Cholesterol Efflux

Alexei V. Navdaev, Lorenzo Sborgi, Samuel D. Wright, Svetlana A. Didichenko

**OBJECTIVE:** To characterize the fate of protein and lipid in nascent HDL (high-density lipoprotein) in plasma and explore the role of interaction between nascent HDL and mature HDL in promoting ABCA1 (ATP-binding cassette transporter 1)-dependent cholesterol efflux.

**APPROACH AND RESULTS:** Two discoidal species, nascent HDL produced by RAW264.7 cells expressing ABCA1 (LpA-I [apo AI containing particles formed by incubating ABCA1-expressing cells with apo AI]), and CSL112, human apo AI (apolipoprotein AI) reconstituted with phospholipids, were used for in vitro incubations with human plasma or purified spherical plasma HDL. Fluorescent labeling and biotinylation of HDL were employed to follow the redistribution of cholesterol and apo AI, cholesterol efflux was measured using cholesterol-loaded cells. We show that both nascent LpA-I and CSL112 can rapidly fuse with spherical HDL. Redistribution of the apo AI molecules and cholesterol after particle fusion leads to the formation of (1) enlarged, remodeled, lipid-rich HDL particles carrying lipid and apo AI from LpA-I and (2) lipid-poor apo AI particles carrying apo AI from both discs and spheres. The interaction of discs and spheres led to a greater than additive elevation of ABCA1-dependent cholesterol efflux.

**CONCLUSIONS:** These data demonstrate that although newly formed discs are relatively poor substrates for ABCA1, they can interact with spheres to produce lipid-poor apo AI, a much better substrate for ABCA1. Because the lipid-poor apo AI generated in this interaction can itself become discoidal by the action of ABCA1, cycles of cholesterol efflux and disc-sphere fusion may result in net ABCA1-dependent transfer of cholesterol from cells to HDL spheres. This process may be of particular importance in atherosclerotic plaque where cholesterol acceptors may be limiting.

**VISUAL OVERVIEW:** An online [visual overview](#) is available for this article.

**Key Words:** apolipoprotein ■ ATP-binding cassette transporter 1 ■ cholesterol ■ lipoprotein ■ phosphatidylcholine

The liver is known to secrete apo AI (apolipoprotein AI) as discoidal nascent HDL (high-density lipoprotein). Discoidal HDL accumulates in the plasma of patients with congenital LCAT (lecithin:cholesterol acyltransferase) deficiency,<sup>1,2</sup> and discoidal forms are found upon perfusion of intact animal livers<sup>3</sup> and after incubation of cholesterol-loaded cells with exogenous apo AI.<sup>4,5</sup> The membrane protein ABCA1 (ATP-binding cassette transporter 1) appears to play an obligate role in formation of discoidal nascent HDL since induction of

ABCA1 dramatically enhances production of discs by cultured cells,<sup>5</sup> and patients with congenital deficiency of ABCA1 have negligible circulating HDL.<sup>6</sup> Discoidal nascent HDL particles are normally short-lived because plasma LCAT acts on discs to produce spherical HDL.<sup>7-10</sup> It has been long assumed that the life cycle of apo AI involves gradual growth from disc to small sphere to large sphere<sup>11,12</sup>; however, recent work has challenged this notion. Mendivil et al<sup>13</sup> demonstrated that HDL of all size classes were observed in the peripheral circulation

Correspondence to: Svetlana A. Didichenko, PhD, CSL Behring AG, Wankdorfstrasse 10, 3014 Bern, Switzerland. Email [svetlana.didichenko@cslobehring.com](mailto:svetlana.didichenko@cslobehring.com)

The Data Supplement is available with this article at <https://www.ahajournals.org/doi/suppl/10.1161/ATVBAHA.120.313906>.

For Sources of Funding and Disclosures, see page 1193.

© 2020 The Authors. *Arteriosclerosis, Thrombosis, and Vascular Biology* is published on behalf of the American Heart Association, Inc., by Wolters Kluwer Health, Inc. This is an open access article under the terms of the [Creative Commons Attribution Non-Commercial-NoDerivs](#) License, which permits use, distribution, and reproduction in any medium, provided that the original work is properly cited, the use is noncommercial, and no modifications or adaptations are made.

*Arterioscler Thromb Vasc Biol* is available at [www.ahajournals.org/journal/atvb](http://www.ahajournals.org/journal/atvb)

## Nonstandard Abbreviations and Acronyms

<b>ABCA1</b>	ATP-binding cassette transporter 1
<b>apo AI</b>	apolipoprotein AI
<b>HDL</b>	high-density lipoprotein
<b>LCAT</b>	lecithin:cholesterol acyltransferase
<b>LpA-I</b>	apo AI containing particles formed by incubating ABCA1-expressing cells with apo AI

at early time points after administration of labeled amino acids to human volunteers, and kinetic analysis of subsequent time points was inconsistent with a model of gradual growth. Additionally, Xu et al<sup>9</sup> showed that esterification of nascent HDL by plasma LCAT is not necessary for the rapid hepatic clearance of free cholesterol from nascent HDL. Further data inconsistent with gradual growth of discs to spheres comes from observations on CSL112, a discoidal particle composed of human apo AI and phosphatidylcholine currently in clinical development for treatment of acute coronary syndrome.<sup>14</sup> Infusion of CSL112 into volunteers lead to rapid elevation of all size classes with a particularly large elevation of lipid-poor apo AI (also known as a HDL-VS [very small HDL] or pre- $\beta$ 1-HDL).<sup>15,16</sup>

Recently, we have described a novel sequence of molecular interactions that underlies the behavior of CSL112 in patients and in plasma.<sup>15</sup> This interaction involves first a fusion of discoidal CSL112 with spherical HDL followed rapidly by a fission event, which results in (1) an enlarged sphere and (2) lipid-poor apo AI. The fission and fusion is a rapid, temperature-dependent process, and it does not require plasma enzymes or remodeling proteins and enzymes, such as LCAT, cholesteryl ester transfer protein, phospholipid transfer protein, hepatic lipase, and endothelial lipase. CSL112 interacts equally well with HDL<sub>2</sub> and HDL<sub>3</sub>. The apo AI in the enlarged remodeled sphere derives from both the parent sphere and from CSL112. Similarly, the apo AI in the lipid-poor apo AI derives from the parent sphere and from CSL112. This sequence of interactions is consistent with all our observations on the behavior of CSL112 upon mixing with purified lipoproteins, whole plasma, or upon infusion into volunteers.<sup>15</sup> The proposed mechanism of remodeling is further supported by early clinical findings with a prototype discoidal particle, CSL111, which showed rapid incorporation of infused apo AI and phospholipids into the endogenous HDL in healthy subjects<sup>17</sup> and in patients with type II diabetes mellitus.<sup>18,19</sup>

CSL112 differs from nascent HDL in that it does not contain cholesterol or lipoproteins other than apo AI. CSL112 contains 2 molecules of apo AI per particle and a defined amount of phospholipid,<sup>14</sup> whereas nascent HDL includes particle species that are diverse in size, apo AI, and lipid content.<sup>4,5,20–25</sup> Therefore, in this study, we asked whether nascent HDL particles (LpA-I [apo AI containing particles

## Highlights

- Here, we demonstrate that both model nascent HDL (high-density lipoprotein) discs formed by ABCA1 (ATP-binding cassette transporter 1)-expressing cells incubated with apo AI (apolipoprotein AI) and HDL discs comprised of human apo AI reconstituted with phosphatidylcholine (CSL112) share the ability to fuse with spherical plasma HDL to generate large cholesterol-rich remodeled spheres and lipid-poor apo AI.
- Lipid-poor apo AI is the primary acceptor of cholesterol from macrophages in the arterial wall, and its availability is likely a limiting factor in cholesterol removal from plaque.
- We propose a model in which nascent HDL discs may act as shuttles between cells and HDL spheres, thus enabling all the HDL particles, not just the smallest species, to participate in reverse cholesterol transport.
- The impact of the interaction between discoidal and spherical HDLs on clinical cardiovascular disease and the potential of discoidal CSL112 to rapidly reduce cholesterol content and stabilize atherosclerotic plaque is now being tested in a large Phase III trial in patients with acute coronary syndrome (AEGIS-II [ApoA-I Event Reducing in Ischemic Syndromes II]).

formed by incubating ABCA1-expressing cells with apo AI]), formed from lipid-free apo AI in a process of cellular lipid efflux mediated by ABCA1, share with CSL112 the ability to fuse with spherical HDL to generate both lipid-poor apo AI and enlarged spheres. We further investigated if this fusion/fission process may play a role in ABCA1-dependent transfer of cellular cholesterol to spherical HDL.

Here, we show that model nascent HDL particles (LpA-I), produced by RAW264.7 cells expressing ABCA1, can rapidly fuse with native plasma HDL with subsequent rapid fission resulting in 2 distinct particle subtypes (1) large, remodeled HDL carrying cholesterol and (2) lipid-poor apo AI particles. Similar to CSL112, the remodeled particles formed by the interaction of LpA-I with plasma HDL have elevated capacity to efflux cholesterol via ABCA1.

## MATERIALS AND METHODS

The authors declare that all supporting data are available within the article.

### Preparation of Reconstituted HDL Formulations

Experimental formulations of reconstituted HDL (Table III in the [Data Supplement](#))<sup>26</sup> were produced using the cholate dialysis method of Matz and Jonas.<sup>27</sup> Briefly, a buffered solution of sodium cholate was used to dissolve the lipids (phosphatidylcholine, sphingomyelin or cholesterol). Soybean phosphatidylcholine was purchased from Phospholipid GmbH (Cologne,

Germany), sphingomyelin from chicken egg yolk, and cholesterol were from Sigma-Aldrich. Lipid solutions were then incubated with plasma-derived apo AI purified as described previously<sup>28</sup> to obtain lipoprotein particles with the required apo AI/lipid molar ratio. Excess cholate was removed by diafiltration. Lipoprotein particles were then concentrated by ultrafiltration to a protein concentration of 20 to 30 mg/mL and lyophilized.

### Isolation of HDL<sub>2</sub> and HDL<sub>3</sub>

HDL<sub>2</sub> ( $d=1.065$ – $1.121$  g/mL) and HDL<sub>3</sub> ( $d=1.13$ – $1.18$  g/mL), were isolated from cryo-depleted plasma (CSL Behring) by sequential ultracentrifugation.<sup>29</sup>

### Protein Labeling

Labeling of HDL<sub>3</sub> with EZ-Link Sulpho-NHS-LC-Biotin or with DyLight 488 Amine-Reactive Dye (both from Pierce Biotechnology) was performed as described previously.<sup>15</sup> Details are described in [Data Supplement](#).

To prepare fluorescent apo AI, CSL112 was labeled with Sulfo-Cy5.5-NHS (Lumiprobe GmbH), as described previously.<sup>15</sup> Labeled CSL112 (40 mg of protein,  $\approx 5$  mg/mL) was delipidated with ethanol/diethyl ether mixture,<sup>30</sup> dissolved in endotoxin-free PBS (Cy5.5–apo AI at 5 mg/mL), and kept at  $-70^{\circ}\text{C}$  until use.

### Preparation of Model Nascent HDL

Murine macrophage RAW264.7 cells were seeded in 150 cm<sup>2</sup> cell culture flasks and grown in DMEM supplemented with 10% (v/v) FBS, 2 mmol/L glutamine, 100 units/mL penicillin, and 100  $\mu\text{g/mL}$  streptomycin in a humidified 37°C incubator in the presence of 5% CO<sub>2</sub>. When cells reached 70% to 80% confluence, the medium was removed, and the cells were loaded with unlabeled 0.2 mmol/L cholesterol (Sigma). Labeling medium was prepared by adding cholesterol dissolved in ethanol at 10 mg/mL to DMEM containing 5% FBS, 2 mmol/L glutamine. After loading with cholesterol for 24 hours, cells were washed with PBS. To upregulate ABCA1, cells were incubated in DMEM/2 mmol/L glutamine/0.2% fatty-acid-free BSA medium containing 0.3 mmol/L 8-bromoadenosine cAMP for 16 hours. Lipid-free apo AI (0.6 mg apo AI per flask) was added to the cells at a final concentration of 20  $\mu\text{g/mL}$  in plain DMEM containing 0.1 mmol/L 8-bromoadenosine cAMP for 24 hours. The resultant LpA-I particles were separated from lipid-free apo AI by density gradient ultracentrifugation at 4°C in a Kontron TFT 70.38 rotor, Hitachi CP100TX centrifuge. Briefly, the density of the cell supernatant was adjusted to 1.18 g/mL and centrifuged for 24 hours at 55 000 rpm (330 000g). The top fraction was collected, concentrated with Ultracel 100K filters, and subjected to size exclusion chromatography on Superose 6 column (2.6 × 70 cm) using an Akta fast protein liquid chromatography system. The LpA-I particles were eluted with PBS, pH 7.4, at a flow rate of 1.5 mL/min. Fractions (4 mL) were collected and analyzed. Relevant fractions were pooled and designated as 1-LpA-I, 2-LpA-I, and 3-LpA-I from the largest to the smallest particle size (Figure 1). LpA-I particles were concentrated by ultrafiltration on Ultracel 100K up to a final protein concentration of 1 to 2 mg/mL. For particle stabilization, sucrose was added up to a final concentration of 1%, and particles were stored in small aliquots (200  $\mu\text{L}$ ) in liquid nitrogen until use. In the majority of the experiments,

unless indicated, 2-LpA-I (designated as LpA-I) was used for the protein labeling and for the incubations with plasma HDL. A similar procedure was used to generate Cy5.5-LpA-I particles.

Cy5.5-LpA-I/TopFluor particles were generated by incubation of TopFluor-cholesterol-labeled RAW264.7 cells with Cy5.5–apo AI. Labeling medium was prepared by complexing the sterols, TopFluor-cholesterol (23-[dipyrrometheneboron difluoride]-24-norcholesterol, Avanti Polar Lipids), and unlabeled cholesterol (Sigma), with methyl- $\beta$ -cyclodextrin (Sigma) at a molar ratio of 1:80 (cholesterol/ $\beta$ -cyclodextrin).<sup>31</sup> Concentrations of TopFluor-cholesterol, unlabeled cholesterol and  $\beta$ -cyclodextrin were 0.025 mmol/L, 0.1 mmol/L and 10 mmol/L, respectively. Labeling of RAW264.7 cells with TopFluor-cholesterol was carried out for 1 hour at 37°C. Except for cell labeling, conditions for cells culture, preparation, and purification of Cy5.5-LpA-I/TopFluor particles were similar to those described for LpA-I.

### Cholesterol Efflux Assay

Cholesterol efflux capacity of different acceptors was assessed using [<sup>3</sup>H]cholesterol-loaded RAW264.7 macrophages as previously described.<sup>14,15</sup> Efflux was promoted by incubating the [<sup>3</sup>H]cholesterol-labeled RAW264.7 cells with each individual acceptor for 5 hours. The difference in efflux between stimulated and nonstimulated cells was taken as a measure of ABCA1-dependent efflux.

### Nondenaturing Polyacrylamide Gradient Gel Electrophoresis, Western Blotting, and Fluorescence Imaging

The HDL particle size distribution was determined by nondenaturing polyacrylamide gradient gel electrophoresis using native 4% to 16% Bis-Tris polyacrylamide gels (Invitrogen by ThermoFisher Scientific). Gels were run at 160 V for 2 hours. Molecular size markers were from GE Healthcare (Amersham High Molecular Weight Calibration Kit for Electrophoresis). Western blotting and fluorescent imaging were performed as described previously.<sup>15</sup> Goat anti-human apo AI polyclonal antibodies (Rockland Immunochemicals Inc) were used for immunodetection of apo AI.

### In Vitro Incubations

Blood was donated voluntarily with signed informed consent under medical supervision. The donation procedure has been approved by an in-house ethical committee led by the medical director. Blood was collected using EDTA-coated tubes (Vacuette, Grenier Bio-One, Austria). To prepare plasma, blood cells are removed by centrifugation for 15 minutes at 2 000 ×g using a refrigerated centrifuge.

Cy5.5-LpA-I was added to fresh human EDTA-plasma at a concentration of 1 mg protein/mL, PBS was added to control plasma sample. Following incubation at 37°C for 0.5 and 1 hour, apoB-containing particles were precipitated from plasma with polyethyleneglycol, as described previously.<sup>15</sup> ApoB-depleted supernatants were used for measurement of cholesterol efflux. The final concentration of Cy5.5-LpA-I added to efflux medium was 5  $\mu\text{g/mL}$ , plasma concentration was 0.5%.

DL488-HDL<sub>3</sub> (fluorescently labeled HDL<sub>3</sub>), B-HDL<sub>3</sub> (biotinylated HDL<sub>3</sub>), LpA-I (1-LpA-I, 2-LpA-I, 3-LpA-I or

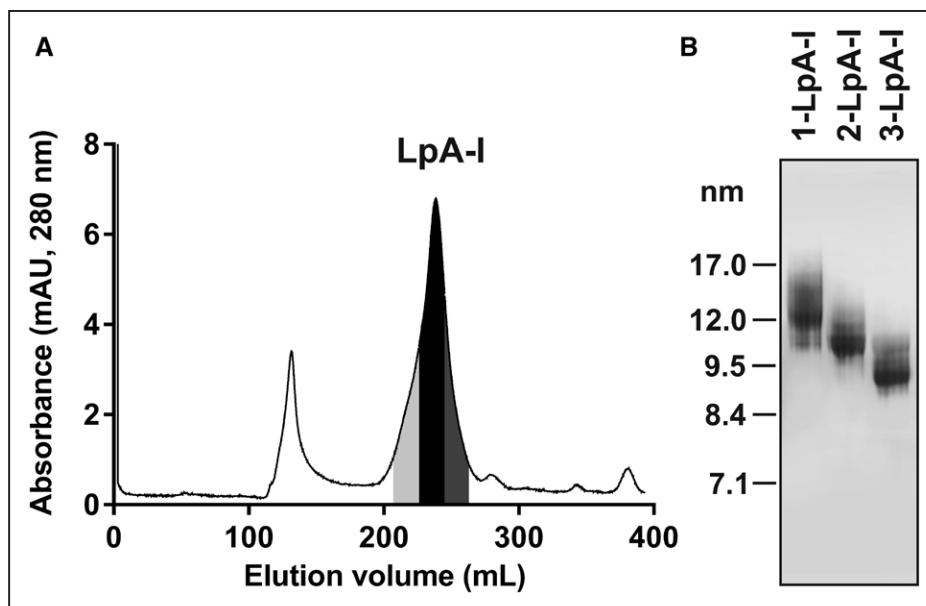


**Figure 1. Purification of nascent LpA-I (apo AI [apolipoprotein AI] containing particles formed by incubating ABCA1 [ATP-binding cassette transporter 1]-expressing cells with apo AI) particles.**

**A**, LpA-I particles were fractionated by size exclusion chromatography on a Superose 6 column. Fractions were collected, pooled as indicated and designated as 1-LpA-I (light gray), 2-LpA-I (black), and 3-LpA-I (dark gray) from the largest to the smallest particle size. **B**, LpA-I subspecies were separated by nondenaturing polyacrylamide gradient gel electrophoresis and visualized by Coomassie Blue G-250 staining. mAU indicates milli absorbance unit.

2-Cy5.5-LpA-I) were used for in vitro incubations as indicated in the figure legends.

Incubation mixtures (80  $\mu$ L) containing biotinylated HDL<sub>3</sub> were incubated with GE Healthcare's Streptavidin Sepharose or Sepharose 4B beads (50  $\mu$ L of the 50% slurry in PBS) with manual gentle mixing. After incubation for 15 minutes at room temperature, the beads were removed by centrifugation, and the supernatants were analyzed.

HDL<sub>3</sub> or HDL<sub>2</sub> (1 mg/mL final concentration) were incubated with increasing concentrations of CSL112 or LpA-I (0.05, 0.1, 0.2, and 0.4 mg protein/mL) in PBS for 1 hour at 37°C. Different formulations of reconstituted HDL (described in the [Data Supplement](#)) were incubated with HDL<sub>3</sub> at 17°C, 37°C, and 50°C as indicated, at a final concentration of each lipoprotein 1 mg/mL.

### Protein and Lipid Analysis, ELISA

Protein concentrations were measured using DC Protein Assay Kit II (Bio-Rad). Phospholipid and total and free cholesterol levels were evaluated enzymatically (LabAssay Phospholipid, LabAssay Cholesterol, and Free Cholesterol E; Wako Diagnostics). Pre $\beta$ <sub>1</sub>-HDL was measured using ELISA kit (Sekisui/American Diagnostica GmbH) according to the manufacturer's recommendations.

Protein conjugate analysis by size exclusion chromatography coupled to multiple angle light scattering was performed as described in the [Data Supplement](#). Data collection and analysis were performed in the ASTRA software using ASTRA's Protein Conjugate Analysis method.<sup>32</sup> The differential refractive index increments (dn/dc) of 0.185, 0.150, and 0.130 were used for molar mass determination of apo AI, phosphatidylcholine and mixture of mammalian lipids, respectively.<sup>33,34</sup>

### Statistics

Values are presented as mean $\pm$ SD. All results were analyzed for statistical significance using 1-way ANOVA followed by Dunnett post hoc test. Statistical significance was set at  $P < 0.05$ . The normality of data and variance were not tested.

## RESULTS

### Characteristics and Composition of Nascent LpA-I Particles

Nascent LpA-I particles were generated by incubation of lipid-free apo AI with ABCA1-expressing RAW 264.7 cells and purified, as described in Materials and Methods. Figure 1A shows the elution profile of LpA-I particles by size exclusion chromatography. For further characterization, peak and side fractions were pooled and designated as 1-LpA-I, 2-LpA-I, and 3-LpA-I. Predominant species in 1-LpA-I, 2-LpA-I, and 3-LpA-I had hydrodynamic diameters of  $\approx 12$  nm,  $\approx 10$  nm, and  $\approx 8.7$  nm, respectively (Figure 1B). Both molar ratios of phospholipid to protein and cholesterol to protein in individual LpA-I species reflected the increase in the average particle size (Table), which is consistent with previous reports.<sup>9,20,21</sup> The phospholipid to protein molar ratio of the smallest nascent 3-LpA-I ( $23.8 \pm 1.7$ ) was comparable to that of purified plasma HDL<sub>2</sub> ( $22.5 \pm 0.2$ ), and for nascent 1-LpA-I and 2-LpA-I species, these ratios were higher ( $28.0 \pm 6.5$  and  $26.9 \pm 6.1$ , respectively). Compared with plasma HDLs, nascent LpA-I particles showed higher levels of cholesterol present in unesterified form (Table). The molar ratio of cholesterol to phospholipid had

**Table. HDL Particle Content of Phospholipid, Total, and Free Cholesterol**

	Ratio		
	Phospholipid: Protein (mol/mol)	Cholesterol: Protein (mol/mol)	Free cholesterol: Protein (mol/mol)
1-LpA-I	28.0±6.5	98.1±8.4	89.3±2.4
2-LpA-I	26.9±6.1	83.3±9.9	76.0±2.3
3-LpA-I	23.8±1.7	62.5±3.5	59.5±0.7
HDL <sub>3</sub>	19.5±1.4	22.5±2.1	4.2±1.2
HDL <sub>2</sub>	22.5±0.2	29.5±3.5	8.2±1.9

The data are shown as mean±SD (n=5). ABCA1 indicates ATP-binding cassette transporter 1; apo AI, apolipoprotein AI; HDL, high-density lipoprotein; and LpA-I, apo AI containing particles formed by incubating ABCA1-expressing cells with apo AI.

a trend to increase with increasing particle size (2.7±0.1 for 3-LpA-I; 3.1±0.3 for 2-LpA-I; and 3.5±0.3 for 1-LpA-I).

## Remodeling of Nascent LpA-I in Human Plasma In Vitro

Remodeling of plasma HDL is a dynamic process which can affect the capacity of the plasma to efflux cellular cholesterol.<sup>35,36</sup> Incubation of LpA-I containing apo AI labeled with Cy5.5 fluorophore (Cy5.5-LpA-I) with normolipidemic plasma caused changes in plasma HDL particle size distribution and led to progressive accumulation

of lipid-poor apo AI (Figure 2A, right). The LpA-I were converted to both smaller and larger particles suggesting that Cy5.5-apo AI became associated with existing plasma HDL. A significant portion of Cy5.5-apo AI was found in a lipid-poor form (Figure 2A, left).

HDL remodeling induced by LpA-I led to changes in plasma capacity to promote cellular cholesterol efflux from RAW264.7 cells. Figure 2B shows that when tested alone, LpA-I and plasma caused comparable cholesterol efflux that was mainly driven by the ABCA1-independent pathway (64% and 59%, respectively), whereas the contribution of the ABCA1-dependent pathway was smaller (36 and 41%, respectively). Incubation of nascent LpA-I with plasma resulted in a sharp increase in the plasma capacity to support ABCA1-dependent cholesterol efflux (≈3-fold increase compared with plasma alone). This finding is consistent with the formation of lipid-poor apo AI, which is the most efficient acceptor of cellular cholesterol via ABCA1.<sup>37</sup>

## In Vitro Remodeling of Nascent LpA-I in the Presence of HDL<sub>3</sub>

Next, we examined the interaction between LpA-I and purified plasma HDL<sub>3</sub>. Cy5.5-LpA-I was incubated with purified plasma HDL<sub>3</sub> labeled with DyLight 488 (DL488-HDL<sub>3</sub>). As shown in Figure 3, both Cy5.5-apo

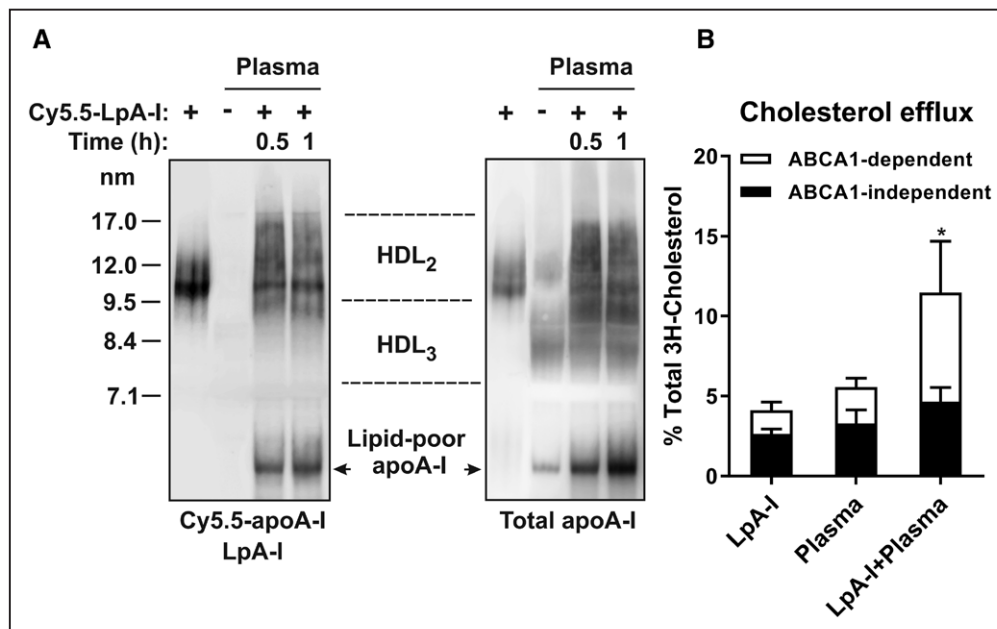


**Figure 2. Effects of nascent LpA-I (apo AI [apolipoprotein AI] containing particles formed by incubating ABCA1 [ATP-binding cassette transporter 1]-expressing cells with apo AI) on the remodeling of endogenous plasma HDL (high-density lipoprotein) and on the plasma cholesterol efflux capacity.**

**A**, Fluorescently labeled nascent LpA-I (Cy5.5-LpA-I) was incubated with human plasma for 0.5 h and 1 h at 37°C. Plasma samples then were separated by nondenaturing polyacrylamide gradient gel electrophoresis, subjected to fluorescence imaging (left; Cy5.5-apo AI) and Western blotting for apo AI (right; total apo AI). The migration positions of HDL<sub>2</sub>, HDL<sub>3</sub>, and lipid-poor apo AI are indicated. **B**, Plasma samples incubated with Cy5.5-LpA-I or PBS for 1 h were used for the measurements of cholesterol efflux from RAW264.7 cells. A sample of LpA-I was included in the analysis as a control. Each efflux value represents the mean±SD for 4 independent experiments performed with different samples measured in triplicate. ABCA1-dependent efflux is presented as the difference in efflux between 8-bromoadenosine cAMP-stimulated and nonstimulated cells. ABCA1-dependent efflux: \*P<0.05 vs plasma.

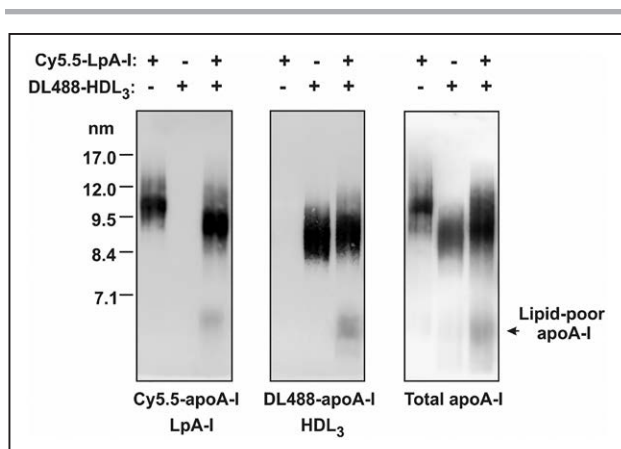


**Figure 3. Lipoprotein particle remodeling is induced by the interaction of nascent LpA-I (apo AI [apolipoprotein AI] containing particles formed by incubating ABCA1 [ATP-binding cassette transporter 1]-expressing cells with apo AI) and HDL<sub>3</sub> in vitro.**

Fluorescently labeled LpA-I (Cy5.5-LpA-I) and HDL<sub>3</sub> (DL488-HDL<sub>3</sub>) were incubated for 1 h at 37°C, final concentration of each lipoprotein was 0.5 mg/mL. Lipoproteins were subjected to nonreducing polyacrylamide gradient gel electrophoresis. Cy5.5-apo AI (left) and DL488-apo AI (middle) were visualized by fluorescent imaging, apo AI (right) was detected by anti-apo AI antibody. The migration of lipid-poor apo AI is also indicated. HDL indicates high-density lipoprotein.

AI and DL488-apo AI from nascent Cy5.5-LpA-I and DL488-HDL<sub>3</sub>, respectively, exhibited similar patterns of association with remodeled HDL species, including lipid-poor apo AI. The majority of the original Cy5.5-LpA-I ( $\approx 10$  nm) was converted to smaller particles ( $\approx 9$ – $9.5$  nm; Figure 3, left), which also accumulated the major portion of DL488-apo AI derived from HDL<sub>3</sub> (Figure 3, middle). Individual changes in LpA-I and HDL<sub>3</sub> particle size distribution detected by fluorescence imaging were consistent with the size distribution of particles detected with anti-apo AI antibody (Figure 3, right). These results suggest that during remodeling, LpA-I associates with HDL<sub>3</sub> giving rise to hybrid particles containing apo AI from both LpA-I and HDL<sub>3</sub>.

### Particle Fusion and Cholesterol Transfer From Nascent LpA-I to HDL Take Place During Particle Remodeling

To investigate whether apo AI derived from LpA-I or HDL<sub>3</sub> resides on the same remodeled particles and whether particle remodeling is accompanied by the transfer of cholesterol between LpA-I particles and HDL, we generated LpA-I (Cy5.5-LpA-I/TopFluor) containing TopFluor-cholesterol as described in Materials and Methods. Cy5.5-LpA-I/TopFluor was then incubated with B-HDL<sub>3</sub>, and the incubation mixtures were treated either with Streptavidin Sepharose beads to capture HDL particles containing biotinylated apo AI or with Sepharose beads (control). As shown in Figure 4, in control mixtures

treated with Sepharose beads, the majority of the remodeled HDL particles had an average particle size of  $\approx 9$  nm. They were smaller than parent Cy5.5-LpA-I/TopFluor ( $\approx 10$  nm) and slightly larger than parent B-HDL<sub>3</sub> ( $\approx 8.7$  nm) as detected with anti-apo AI antibody (Figure 4A). The main portion of both biotinylated apo AI and Cy5.5-apo AI (Figure 4D and 4B, respectively), and all detected TopFluor-cholesterol (Figure 4C) were associated with these remodeled particles. The lipid-poor apo AI fraction contained biotinylated apo AI and Cy5.5-apo AI (Figure 4D and 4B) but no trace of TopFluor-cholesterol (Figure 4C). Precipitation with Streptavidin Sepharose beads removed, from the incubation mixtures, all biotinylated apo AI together with the majority of Cy5.5-apo AI and TopFluor-cholesterol, indicating that apo AI from LpA-I and apo AI from HDL<sub>3</sub> are present on the same remodeled particles (see confirming studies in Figure 1 in the Data Supplement). A small amount of Cy5.5-LpA-I/TopFluor particles ( $\approx 10$  nm and  $\approx 9$  nm) remained in the incubation mixture after removal of biotinylated apo AI (Figure 4A and 4B). Smaller Cy5.5-LpA-I/TopFluor particles contained much less TopFluor-cholesterol compared with nonremodeled parent Cy5.5-LpA-I/TopFluor (Figure 4C) suggesting that a net transfer of cholesterol from nascent 2-LpA-I to HDL<sub>3</sub> contributes to their formation. In conclusion, these data support the concept of fusion between LpA-I and HDL<sub>3</sub>, followed by structural rearrangements and the dissociation of apo AI. Additionally, particle remodeling is accompanied by the movement of cholesterol between the particles.

### Particle Remodeling Between Nascent LpA-I and HDL<sub>3</sub> Leads to the Enhancement of Cholesterol Efflux

To evaluate the effects of the particle remodeling on HDL functionality, we measured the cholesterol efflux capacities of the remodeled HDL particles generated upon in vitro incubation of 1-LpA-I, 2-LpA-I or 3-LpA-I with HDL<sub>3</sub> using corresponding parent particles and apo AI for direct comparison. Figure 5 demonstrates that when tested alone, all nascent LpA-I species showed comparable capacity to efflux cholesterol. Similar to HDL<sub>3</sub>, they were more efficient acceptors of cellular cholesterol via the ABCA1-independent pathway. With decreasing LpA-I particle size, the contribution of ABCA1-dependent efflux increased but was much less than that of the apo AI comparator. These observations are consistent with prior work suggesting that nascent LpA-I are both products of and substrates for ABCA1 and that the level of lipidation of LpA-I determines their ability for subsequent interaction with ABCA1.<sup>38</sup>

Incubation of HDL<sub>3</sub> with 1-LpA-I, 2-LpA-I or 3-LpA-I significantly increased (1.7- to 4-fold) the potential of remodeled HDL species to efflux cellular cholesterol via ABCA1 (Figure 5) in comparison to corresponding

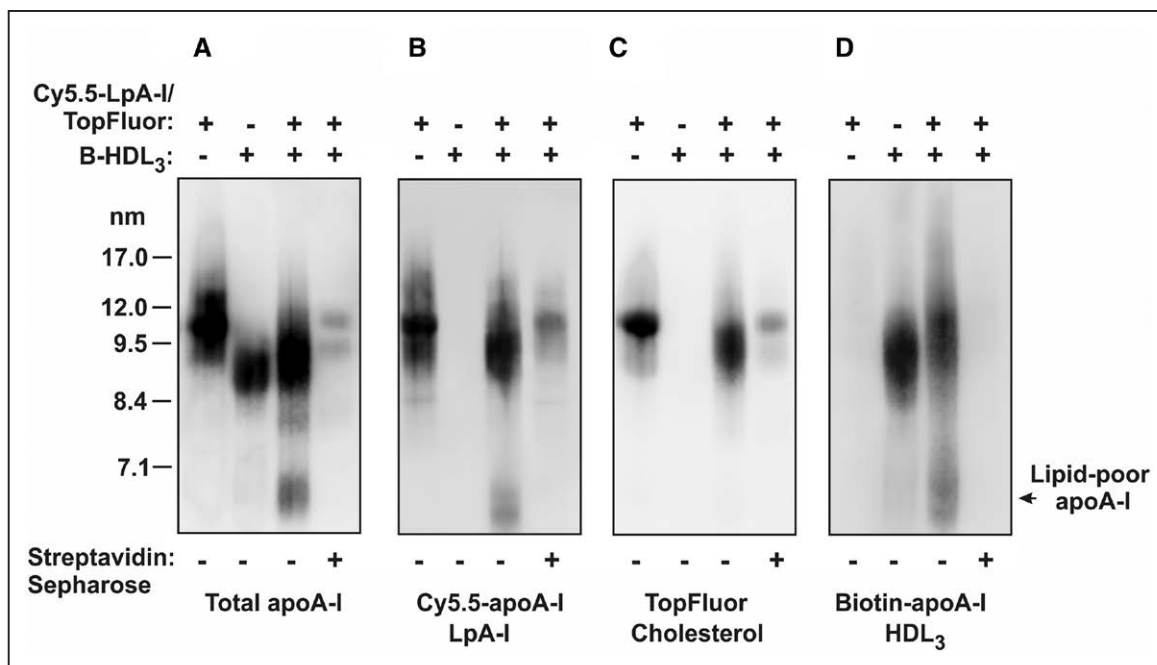


**Figure 4. Cholesterol transfer between nascent LpA-I (apo AI [apolipoprotein AI]) containing particles formed by incubating ABCA1 [ATP-binding cassette transporter 1]-expressing cells with apo AI) and HDL<sub>3</sub> takes place during particle remodeling in vitro.**

Cy5.5-LpA-I/TopFluor particles containing TopFluor-cholesterol were incubated with B-HDL<sub>3</sub> (biotinylated HDL<sub>3</sub>) for 1 h at 37°C, final concentration of each lipoprotein was 0.5 mg/mL. Following treatment of the reaction mixtures with Sepharose beads (–) or Streptavidin Sepharose beads (+), lipoproteins remained in the supernatants were separated by nondenaturing polyacrylamide gradient gel electrophoresis. apo AI (A) and biotinylated apo AI (D) were detected with anti-apo AI antibody and NeutrAvidin, respectively. Cy5.5-apo AI (B) and TopFluor-cholesterol (C) were visualized by fluorescent imaging. The position of migration of lipid-poor apo AI is indicated. HDL, high-density lipoprotein

parent LpA-I species, whereas an increase in ABCA1-independent efflux was less prominent (1.3- to 2.2-fold).

LpA-I formed by ABCA1-expressing murine macrophage RAW264.7 cells have been shown to possess a discoidal morphology.<sup>5</sup> To estimate the potential impact of disc- sphere remodeling in normal physiology, we explored conditions which may more closely reflect those seen in humans. Given that plasma contains very low levels of discoidal HDL,<sup>11,39,40</sup> we induced HDL remodeling in vitro using graded concentrations of discs (LpA-I or CSL112) in the presence of an amount of HDL<sub>2</sub> or HDL<sub>3</sub> comparable to that in normal human plasma. Then we sought to mimic the conditions near cholesterol-laden, ABCA1-expressing cells outside the vasculature, where lipoprotein levels are about 5-fold reduced compared to blood levels.<sup>40–42</sup>

HDL<sub>3</sub> or HDL<sub>2</sub> (at 1 mg protein/ mL) were incubated with increasing concentrations of nascent LpA-I or CSL112 (0.05, 0.1, 0.2, and 0.4 mg/mL apo AI) for 1 hour at 37°C. Then the incubation mixtures were used as cholesterol acceptors at a low final HDL<sub>3</sub> or HDL<sub>2</sub> concentration (10 µg protein/mL) to measure cholesterol efflux from RAW264.7 cells expressing ABCA1. Figure 6 shows that under experimental conditions in which macrophage cells were in excess and the concentration of HDL<sub>2</sub> or HDL<sub>3</sub> (10 µg/mL) was a limiting factor for cholesterol efflux, addition of lower levels of discs, LpA-I

(≥2 µg) or CSL112 (≥1 µg), elevated ABCA1-dependent efflux to a greater than additive extent (Figure 6A and 6B, respectively; Table I in the [Data Supplement](#)). CSL112 appeared more effective than nascent LpA-I in synergistically elevating ABCA1-dependent efflux; this difference may be related to levels of lipid-poor apo AI produced upon HDL remodeling. CSL112 produced more lipid-poor apo AI than LpA-I when incubated with HDL<sub>2</sub> or HDL<sub>3</sub> at the same low concentration of 0.2 mg protein/mL (Figure 6C). Larger production of lipid-poor apo AI by CSL112 was seen even upon doubling the protein concentration of LpA-I to 0.4 mg protein/mL (Figure 6C), which corresponds to approximately similar phospholipid and particle concentration as CSL112<sup>14</sup> at 0.2 mg protein/mL (Table; Figure II and Table II in the [Data Supplement](#)).

Taken together, these data suggest a synergistic action of discs and spheres to enable ABCA1-dependent efflux and show that the efficiency of the formation of lipid-poor apo AI upon remodeling depends on the disc size, structure and lipid composition. The structure of spherical HDL also appeared to play a role in the process of particle remodeling with greater production of lipid-poor apo AI deriving from smaller HDL<sub>3</sub> versus larger HDL<sub>2</sub> (Figure 6C). This is consistent with observations that apo AI interacts much more readily with HDL<sub>3</sub> than with large HDL<sub>2</sub>.<sup>43</sup>

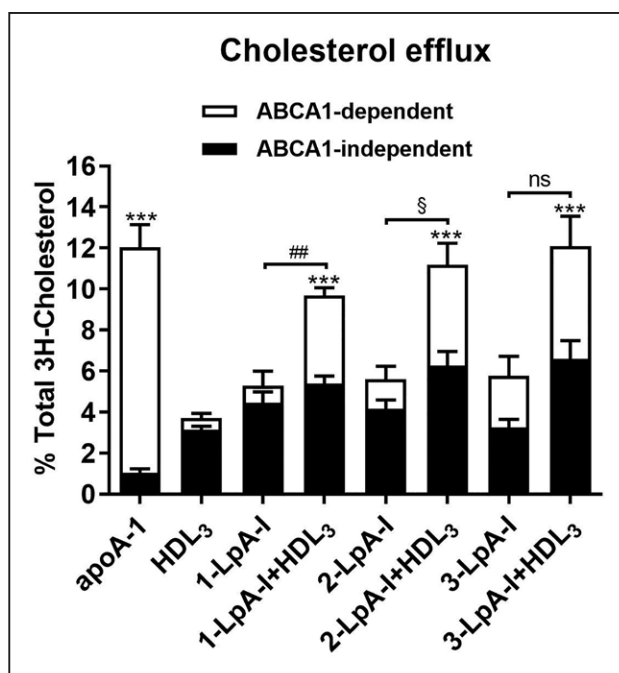


**Figure 5. Particle remodeling between nascent LpA-I (apo AI [apolipoprotein AI] containing particles formed by incubating ABCA1 [ATP-binding cassette transporter 1]-expressing cells with apo AI) and HDL<sub>3</sub> leads to the enhancement of the cholesterol efflux.**

1-LpA-I, 2-LpA-I or 3-LpA-I were incubated with HDL<sub>3</sub> for 1 h at 37°C (at a final concentration of 0.5 mg/mL of each lipoprotein). The LpA-I, HDL<sub>3</sub>, and apo AI incubated alone in PBS were included as controls. Incubation mixtures were used for the measurements of cholesterol efflux from RAW264.7 cells. The final concentration of cholesterol acceptors in efflux medium was 10 µg/mL. Each efflux value represents the mean±SD for 3 independent experiments performed with different samples measured in triplicate. HDL, high-density lipoprotein. ABCA1-dependent efflux: \*\*\* $P$ <0.001, \*\* $P$ <0.01, \* $P$ <0.05 vs HDL<sub>3</sub>; ## $P$ <0.01, vs 1-LpA-I; S $P$ <0.05, vs 2-LpA-I; ns (nonsignificant) difference vs 3-LpA-I.

### Lipid Content and Size of Lipoproteins Influence Generation of Lipid-Poor apo AI Upon Interaction of Discs With Spheres

To understand the physical determinants driving the remodeling reaction here, we used a series of well-defined formulations of reconstituted lipoproteins<sup>26</sup> (Table III in the [Data Supplement](#)), each of which contains 2 molecules of apo AI per particle, to show the influence of lipid amount and identity on apo AI release upon interaction with HDL (Figure 7). Increasing the phosphatidylcholine levels from a molar ratio of phosphatidylcholine 32:1 apo AI to a molar ratio of phosphatidylcholine 100:1 apo AI caused a graded reduction in lipid-poor apo AI production, and further addition of cholesterol caused further reduction of lipid-poor apo AI production. Similar findings were seen whether lipid-poor apo AI was measured by gel electrophoresis or by immunoassay (Figure 7A and 7B). Substitution of the phosphatidylcholine with sphingomyelin in HDL (sphingomyelin 100:1 apo AI) reduced lipid-poor apo AI release at 17°C and 37°C, but similar

release was seen upon elevation of temperature to 50°C (Figure 7C and 7D). These data suggest the gel-to-liquid crystalline phase transition temperature of the phospholipid affects remodeling, with inhibition near or below that temperature<sup>44</sup> but that above this temperature, the amount of lipid is a critical parameter.

## DISCUSSION

Earlier published work on model nascent HDL particles has documented their interaction with spherical HDL. Injection of LpA-I into rabbits<sup>36</sup> and into human apo AI transgenic mice<sup>45</sup> resulted in a rapid changes in the LpA-I size distribution following interaction with pre-existing endogenous HDL. Furthermore, Bailey et al<sup>36</sup> showed that the free cholesterol content of injected [<sup>3</sup>H] free cholesterol-radiolabeled reconstituted HDL was rapidly redistributed to rabbit HDL and low-density lipoprotein. Recently, Xu et al<sup>9</sup> demonstrated the transfer of [<sup>3</sup>H]free cholesterol, [<sup>14</sup>C]phospholipid, and [<sup>125</sup>I]apo AI contents of LpA-I particles to plasma HDL and low-density lipoprotein in vitro.<sup>9</sup> In the present study, we corroborate these findings and describe additional steps in HDL biogenesis. We show that LpA-I particles generated by ABCA1-expressing RAW264.7 cells spontaneously fuse with spherical plasma HDL in vitro. Subsequent fission of the fusion product leads to 2 novel species: HDL spheres of enlarged size and lipid-poor apo AI (Figures 2 through 4, and 6C). In this process, LpA-I first donates both apo AI and lipid to the spherical HDL, and in the subsequent fission, lipid-free apo AI from both the spherical HDL and the LpA-I is released into the medium. Plasma factors, such as phospholipid transfer protein, cholesterol ester transfer protein, or LCAT, are known to contribute to HDL remodeling in some contexts, but we found they are not essential for the particle remodeling studied here because LpA-I is able to induce HDL remodeling and lipid-poor apo AI release in plasma of wild-type mice, which are naturally cholesterol ester transfer protein-deficient as well as in plasma from mice deficient in phospholipid transfer protein or LCAT (Figure III in the [Data Supplement](#)). The sequence of events we document here for LpA-I closely resembles the sequence we established for CSL112, a discoidal particle composed of human apo AI and phosphatidylcholine.<sup>15</sup> These studies also showed transient fusion of CSL112 discs with HDL spheres and subsequent fission to yield lipid-poor apo AI. These common features of HDL particle remodeling induced by LpA-I and CSL112 suggest a general mechanism by which spontaneous interaction between spherical and discoidal HDL leads to generation of lipid-poor apo AI making it available for additional cycles of tissue cholesterol efflux (Figure 8).

Particle size and composition of discoidal and spherical HDLs appear to be critical parameters controlling the levels of lipid-poor apo AI produced during remodeling.



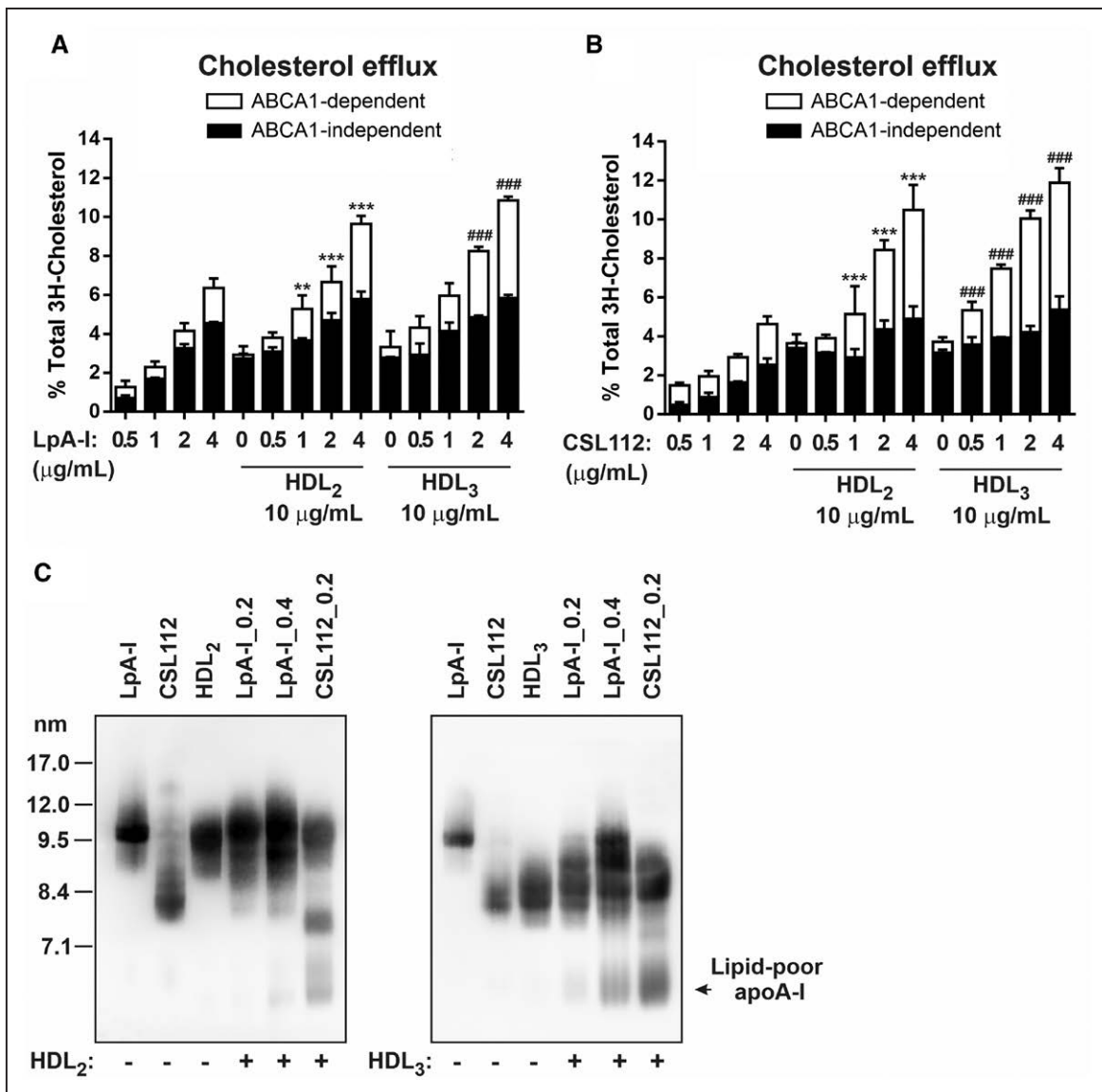


**Figure 6.** Small discoidal CSL112 induces more lipid-poor apo AI (apolipoprotein AI) upon incubation with HDL (high-density lipoprotein) compared with the nascent LpA-I (apo AI containing particles formed by incubating ABCA1 [ATP-binding cassette transporter 1]-expressing cells with apo AI).

HDL<sub>3</sub> or HDL<sub>2</sub> (final protein concentration 1 mg/mL) were incubated for 1 h at 37°C in the absence or presence of increasing concentrations of LpA-I or CSL112 (at 0.05, 0.1, 0.2, and 0.4 mg protein/mL). Cholesterol efflux from RAW264.7 macrophages is shown (A and B). Final concentrations of LpA-I (A) or CSL112 (B) in efflux medium were 0.5, 1, 2, and 4 μg protein/mL; HDL<sub>3</sub> or HDL<sub>2</sub> were at 10 μg protein/mL, as indicated. Data from three independent experiments are shown. Values are presented as mean±SD. ABCA1-dependent efflux: \*\*\* $P$ <0.001, \*\* $P$ <0.01 vs HDL<sub>2</sub>; ### $P$ <0.001 vs HDL<sub>3</sub>. C, HDL<sub>2</sub> or HDL<sub>3</sub> (final protein concentration 1 mg/mL) were incubated with LpA-I (0.2 and 0.4 mg/mL final protein concentrations; [LpA\_0.2] and [LpA\_0.4], respectively) or CSL112 (final protein concentration 0.2 mg/mL; [CSL112\_0.2]) for 1 h at 37°C. Lipoproteins were separated by nondenaturing polyacrylamide gradient gel electrophoresis, and apo AI was detected by anti-apo AI antibody. The migration of lipid-poor apo AI is indicated.

Increasing size and lipid content of discs appear to reduce formation of lipid-poor apo AI during remodeling (Figure 6C and Figure 7A), and increasing size of spheres also appears to reduce production of lipid-poor apo AI during remodeling (Figure 6C). The stability of the interaction of apo AI with lipid is likely to dictate its propensity to disassociate as a lipid-poor species, and further study of the energetics of the formation of lipid-poor apo AI during disc-sphere interaction is warranted. At a

simple level, our results are consistent with the notion that particles with less or insufficient surface lipid may allow ready disassociation.

Two distinct physiological consequences of the interaction of discs with spheres may be observed in two locations in the body. In the liver, which produces nascent HDL from newly synthesized apo AI, discs are fed into the perisinusoidal space of Disse before passing into the circulation. The plentiful HDL spheres in circulation likely

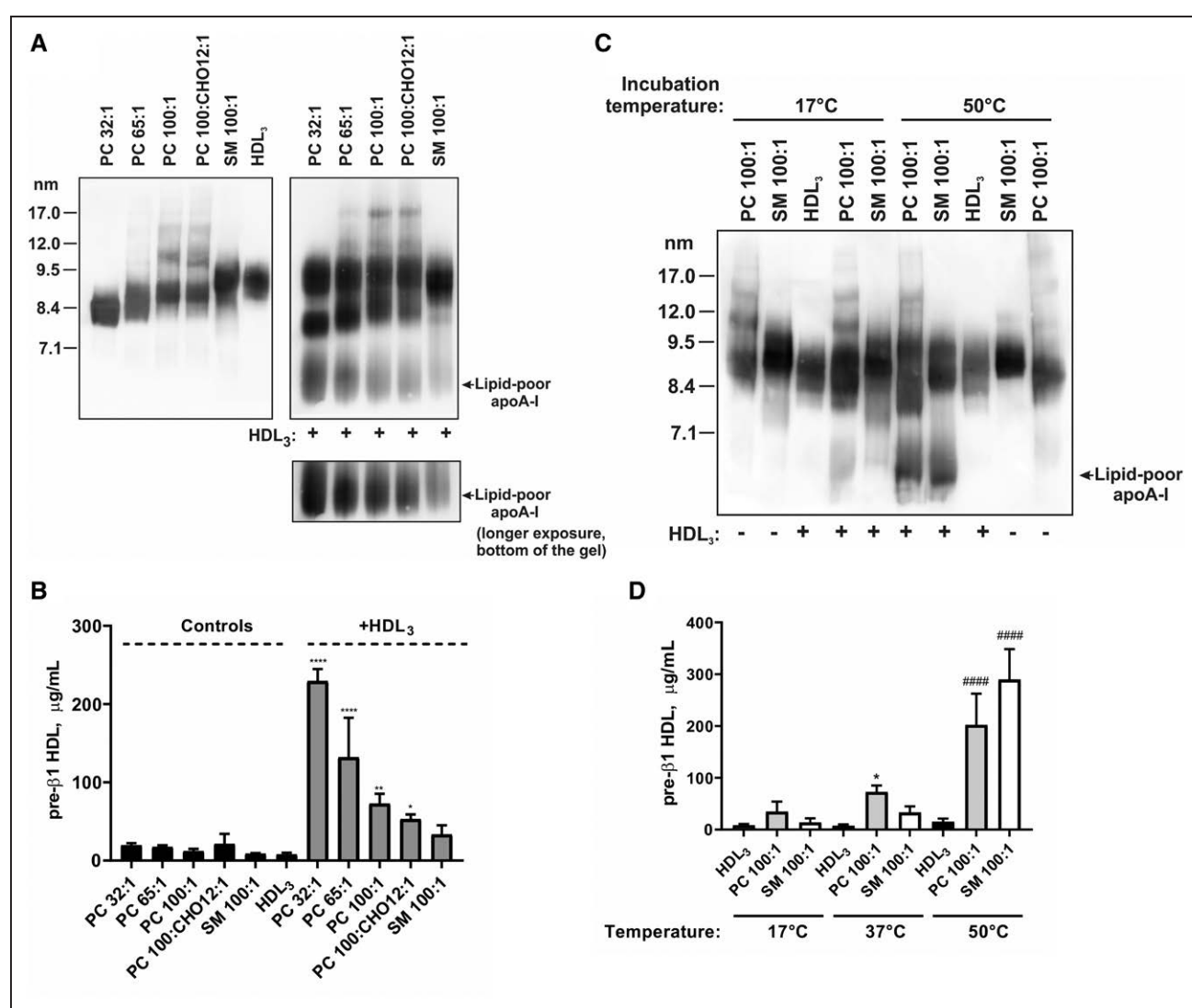


**Figure 7. Phospholipid:protein ratio and lipid composition of discoidal HDLs (high-density lipoproteins) impact on interaction with HDL<sub>3</sub> and apo AI (apolipoprotein AI) release.**

HDL<sub>3</sub> (final protein concentration 1 mg/mL) was incubated for 1 h with different formulations of reconstituted HDL (final protein concentration 1 mg/mL) as indicated. Formulations of reconstituted HDL are described in Table II in the [Data Supplement](#). Lipid-poor apo AI was analyzed either by Western blotting with anti-apo AI antibody following separation of lipoproteins by nondenaturing polyacrylamide gradient gel electrophoresis (**A** and **C**) or by pre-β1 HDL ELISA (**B** and **D**). Lipoproteins incubated alone in PBS were included as controls. **A** and **B**, Incubation at 37°C. **C**, Incubation at 17°C and 50°C. **D**, Shown data for incubations of HDL<sub>3</sub> with phosphatidylcholine (PC) 100:1 apo AI (gray bars) and sphingomyelin (SM) 100:1 apo AI (white bars) at 17°C, 37°C and 50°C. **B** and **D**, Data from three independent experiments are shown. Values are presented as mean±SD. **B**, Pre-β1: \*\*\*\* $P < 0.0001$ , \*\*\* $P < 0.001$ , \*\* $P < 0.01$ , \* $P < 0.05$  vs HDL<sub>3</sub>. **D**, Pre-β1: #### $P < 0.0001$  and \* $P < 0.05$  vs HDL<sub>3</sub>, for incubations at 50°C and 37°C, respectively.

drive a very rapid interaction with the newly formed discs. Indeed, Mendivil et al. have observed virtually no labeled discs in the peripheral circulation 120 minutes after the addition of labeled amino acids to human volunteers.<sup>13</sup> Rather, the newly synthesized apo AI was found in a full spectrum of HDL sizes, as predicted by our observations. Lipid-rich, large, remodeled spheres produced upon interaction of nascent HDL discs and spherical HDL could enter pathways for cholesterol clearance.

The second location in which disc-sphere interactions may be critical is in the interstitial fluid surrounding foam cells of an atheroma. In this location, the amount

of substrate for ABCA1 is likely to be the main feature that limits the exit of cholesterol. The most important contributor to this condition is the very high volume of cholesterol-laden cells versus the low volume of interstitial fluid that can receive the cholesterol. Additional factors limiting efflux in plaque are the low concentration of HDL in interstitial fluid (20% of plasma levels)<sup>46,47</sup> and the inability of mature HDL spheres and lipid-rich discs to interact with ABCA1 (Figures 5 and 6).<sup>38</sup> Finally, the oxidative and inflammatory environment in the plaque may further diminish the ability of local apo AI to interact with ABCA1.<sup>48–50</sup> Thus, the interaction of

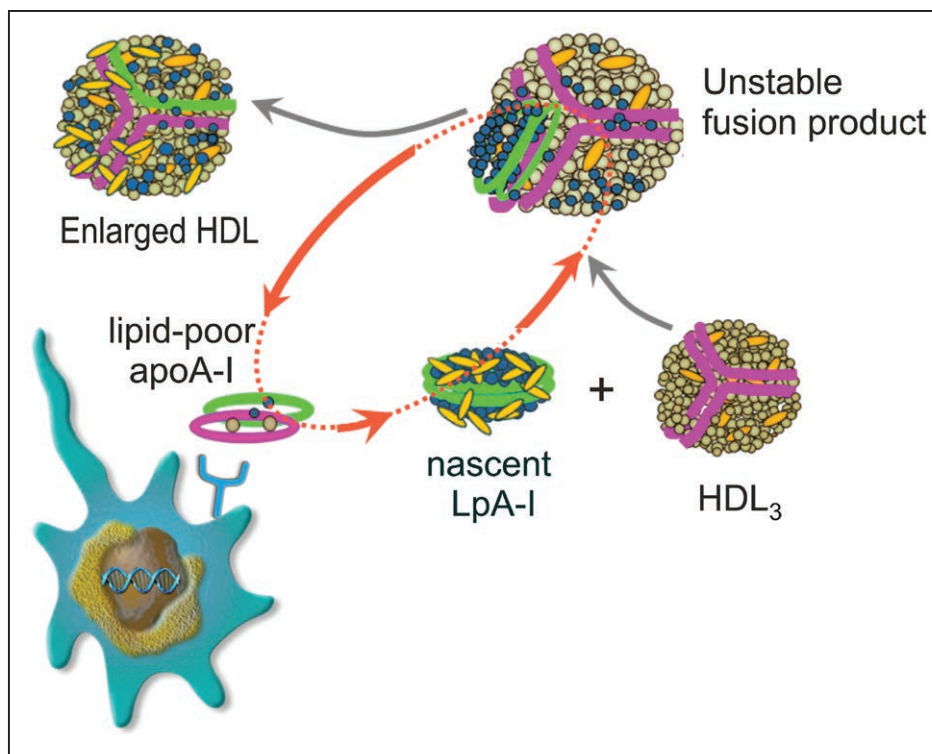


**Figure 8. Shuttle model for discs in ABCA1 (ATP-binding cassette transporter 1)-dependent transport of cholesterol to HDL (high-density lipoprotein).**

Nascent LpA-I (apo AI [apolipoprotein AI] containing particles formed by incubating ABCA1-expressing cells with apo AI) discs are formed by ABCA1-mediated efflux of cellular cholesterol and phospholipids to lipid-poor apo AI. Nascent LpA-I can interact with HDL in the interstitial fluid, shuttling cholesterol and phospholipid into HDL. This interaction may lead to the particle fusion and subsequent shedding of apo AI from the remodeled large fusion product to yield new lipid-poor apo AI. Phospholipids in LpA-I and HDL<sub>3</sub> are colored in blue and light brown, respectively. Apo AI molecules are shown in green (LpA-I) and purple (HDL<sub>3</sub>); cholesterol is shown in yellow.

discs with spheres described here may help close a gap in the understanding of cholesterol transport from the atheroma. Discs formed locally by the action of ABCA1 expressed on foam cells may fuse with nearby spheres to both transfer cholesterol to the spheres and generate more lipid-free apo AI, and thereby more acceptors for ABCA1-dependent efflux. As this process cycles, the discs may act as shuttles between cells and HDL spheres, thus enabling all the HDL particles, not just the smallest species, to participate in cholesterol transport (Figure 8). In support of this, we have observed that addition of a small amount of discs to a larger portion of spheres causes a greater than additive rise in ABCA1-dependent cholesterol efflux (Figures 6 and Table I in the [Data Supplement](#)). The ability of discs to enhance cholesterol efflux under conditions in which the availability of ABCA1 substrate is a limiting factor suggests a mechanism underlying the strong reduction of plaque cholesterol observed upon infusion of apo AI discs. As previously noted,<sup>14</sup> more than half of plaque cholesterol ester can be removed in two weeks after infusion of apo AI discs into rabbits,<sup>51</sup> mice,<sup>52</sup> or man.<sup>53</sup> The potential to rapidly reduce cholesterol content and stabilize atherosclerotic plaque is now being tested in AEGIS-II

(ApoA-I Event Reducing in Ischemic Syndromes II), a large Phase III trial of CSL112.<sup>54</sup>

In recent years, 2 different formulations of apo AI, MDC0216 and CER001, showed disappointing results in clinical trials with plaque imaging end points.<sup>55,56</sup> It is likely that multiple factors contributed to this failure. The intravascular ultrasound imaging methods used in these trials depict plaque size but not plaque stability, and recent animal studies have shown that apo AI may strongly reduce plaque cholesterol and macrophage content and elevate plaque collagen without net changes in plaque size.<sup>50</sup> The end points chosen may thus have been insensitive to the effects of the drugs. The failed trials also used relatively low doses of apo AI.<sup>57</sup> But in the context of the current findings, it is noteworthy that CER001 was composed of sphingomyelin, a lipid which may not optimally support the remodeling described here (Figure 7) and which inhibits LCAT, the second step of reverse cholesterol transport.<sup>58</sup> MDC0216 was composed with dimeric apo AI Milano, a mutant version of apo AI, which fails to activate LCAT,<sup>59</sup> causes hypercatabolism of endogenous apo AI<sup>60</sup> and does not form lipid-poor apo AI during remodeling<sup>61</sup> as seen with CSL112 (Figure 6C). The ongoing AEGIS-II trial of CSL112 employs a major adverse cardiac event end point and may avoid the above issues.

A key limitation of this study is that the HDL remodeling was studied using a static in vitro cell-free system, and the contribution of HDL-low-density lipoprotein and HDL-cell interactions on the process was not assessed. This study describes the effects of spontaneous interaction between discoidal and spherical HDL particles, independent of LCAT, cholesterol ester transfer protein, and phospholipid transfer protein. The role of other factors, such as hepatic lipase and endothelial lipase, that are known to affect HDL remodeling, were not investigated. Additionally, besides cholesterol efflux, we did not explore other functional properties of the remodeled HDL particles, which can be atheroprotective (ie, anti-inflammatory and antioxidant).

In conclusion, our findings provide a biochemical description of the pathway for nascent HDL remodeling and insights into the mechanism of interaction between discoidal and spherical HDLs. The proposed model supports the hypothesis that lipid-poor apo AI, the primary acceptor of the cholesterol that is exported from cells via ABCA1, can be locally produced in close vicinity to atherosclerotic plaque, initiate de novo ABCA1-dependent cholesterol efflux from macrophages and thereby contribute to the removal of excess cell cholesterol and improvement in plaque composition and possibly stability.

## ARTICLE INFORMATION

Received August 1, 2019; accepted February 5, 2020.

### Affiliations

From the CSL Behring AG, Bern, Switzerland (A.V.N., L.S., S.A.D.); and CSL Behring, King of Prussia, PA (S.D.W.).

### Acknowledgments

We would like to thank Dr T. Heck for providing reconstituted HDL (high-density lipoprotein) formulations and Dr B. Kingwell and Dr K. Rye for careful reading of the article and critical comments.

### Sources of Funding

This work was funded by CSL Behring.

### Disclosures

A.V. Navdaev, L. Sborgi, S.D. Wright, and S.A. Didichenko are employees of CSL Behring.

## REFERENCES

- Norum KR, Glomset JA, Nichols AV, Forte T. Plasma lipoproteins in familial lecithin: cholesterol acyltransferase deficiency: physical and chemical studies of low and high density lipoproteins. *J Clin Invest*. 1971;50:1131–1140. doi: 10.1172/JCI106585
- Forte T, Norum KR, Glomset JA, Nichols AV. Plasma lipoproteins in familial lecithin: cholesterol acyltransferase deficiency: structure of low and high density lipoproteins as revealed by electron microscopy. *J Clin Invest*. 1971;50:1141–1148. doi: 10.1172/JCI106586
- Hamilton RL, Williams MC, Fielding CJ, Havel RJ. Discoidal bilayer structure of nascent high density lipoproteins from perfused rat liver. *J Clin Invest*. 1976;58:667–680. doi: 10.1172/JCI108513
- Duong PT, Collins HL, Nickel M, Lund-Katz S, Rothblat GH, Phillips MC. Characterization of nascent HDL particles and microparticles formed by ABCA1-mediated efflux of cellular lipids to apoA-I. *J Lipid Res*. 2006;47:832–843. doi: 10.1194/jlr.M500531-JLR200
- Lyssenko NN, Nickel M, Tang C, Phillips MC. Factors controlling nascent high-density lipoprotein particle heterogeneity: ATP-binding cassette transporter A1 activity and cell lipid and apolipoprotein AI availability. *FASEB J*. 2013;27:2880–2892. doi: 10.1096/fj.12-216564
- Singaraja RR, Brunham LR, Visscher H, Kastelein JJ, Hayden MR. Efflux and atherosclerosis: the clinical and biochemical impact of variations in the ABCA1 gene. *Arterioscler Thromb Vasc Biol*. 2003;23:1322–1332. doi: 10.1161/01.ATV.0000078520.89539.77
- Zannis VI, Chroni A, Krieger M. Role of apoA-I, ABCA1, LCAT, and SR-BI in the biogenesis of HDL. *J Mol Med (Berl)*. 2006;84:276–294. doi: 10.1007/s00109-005-0030-4
- Zannis VI, Su S, Fotakis P. Role of apolipoproteins, ABCA1 and LCAT in the biogenesis of normal and aberrant high density lipoproteins. *J Biomed Res*. 2017;31:471–485. doi: 10.7555/JBR.31.20160082
- Xu B, Gillard BK, Gotto AM Jr, Rosales C, Pownall HJ. ABCA1-derived nascent high-density lipoprotein-apoA-I and lipids metabolically segregate. *Arterioscler Thromb Vasc Biol*. 2017;37:2260–2270. doi: 10.1161/ATVBAHA.117.310290
- Glomset JA. The plasma lecithins:cholesterol acyltransferase reaction. *J Lipid Res*. 1968;9:155–167.
- Rothblat GH, Phillips MC. High-density lipoprotein heterogeneity and function in reverse cholesterol transport. *Curr Opin Lipidol*. 2010;21:229–238. doi: 10.1097/mol.0b013e328338472d
- Toth PP, Barter RJ, Rosenson RS, Boden WE, Chapman MJ, Cuchel M, D'Agostino RB Sr, Davidson MH, Davidson WS, Heinecke JW, et al. High-density lipoproteins: a consensus statement from the National Lipid Association. *J Clin Lipidol*. 2013;7:484–525. doi: 10.1016/j.jacl.2013.08.001
- Mendivil CO, Furtado J, Morton AM, Wang L, Sacks FM. Novel pathways of apolipoprotein A-I metabolism in high-density lipoprotein of different sizes in humans. *Arterioscler Thromb Vasc Biol*. 2016;36:156–165. doi: 10.1161/ATVBAHA.115.306138
- Didichenko S, Gille A, Pragst I, Stadler D, Waelchli M, Hamilton R, Leis A, Wright SD. Novel formulation of a reconstituted high-density lipoprotein (CSL112) dramatically enhances ABCA1-dependent cholesterol efflux. *Arterioscler Thromb Vasc Biol*. 2013;33:2202–2211. doi: 10.1161/ATVBAHA.113.301981
- Didichenko SA, Navdaev AV, Cukier AM, Gille A, Schuetz P, Spycher MO, Théron P, Chapman MJ, Kontush A, Wright SD. Enhanced HDL functionality in small HDL species produced upon remodeling of HDL by reconstituted HDL, CSL112: effects on cholesterol efflux, anti-inflammatory and antioxidative activity. *Circ Res*. 2016;119:751–763. doi: 10.1161/CIRCRESAHA.116.308685
- Rosenson RS, Brewer HB Jr, Chapman MJ, Fazio S, Hussain MM, Kontush A, Krauss RM, Otvos JD, Remaley AT, Schaefer EJ. HDL measures, particle heterogeneity, proposed nomenclature, and relation to atherosclerotic cardiovascular events. *Clin Chem*. 2011;57:392–410. doi: 10.1373/clinchem.2010.155333
- Nanjee MN, Doran JE, Lerch PG, Miller NE. Acute effects of intravenous infusion of ApoA1/phosphatidylcholine discs on plasma lipoproteins in humans. *Arterioscler Thromb Vasc Biol*. 1999;19:979–989. doi: 10.1161/01.atv.19.4.979
- Patel S, Drew BG, Nakhla S, Duffy SJ, Murphy AJ, Barter RJ, Rye KA, Chin-Dusting J, Hoang A, Sviridov D, et al. Reconstituted high-density lipoprotein increases plasma high-density lipoprotein anti-inflammatory properties and cholesterol efflux capacity in patients with type 2 diabetes. *J Am Coll Cardiol*. 2009;53:962–971. doi: 10.1016/j.jacc.2008.12.008
- Hoang A, Drew BG, Low H, Remaley AT, Nestel P, Kingwell BA, Sviridov D. Mechanism of cholesterol efflux in humans after infusion of reconstituted high-density lipoprotein. *Eur Heart J*. 2012;33:657–665. doi: 10.1093/eurheartj/ehr103
- Sorci-Thomas MG, Owen JS, Fulp B, Bhat S, Zhu X, Parks JS, Shah D, Jerome WG, Gerelus M, Zabalawi M, et al. Nascent high density lipoproteins formed by ABCA1 resemble lipid rafts and are structurally organized by three apoA-I monomers. *J Lipid Res*. 2012;53:1890–1909. doi: 10.1194/jlr.M026674
- Duong PT, Weibel GL, Lund-Katz S, Rothblat GH, Phillips MC. Characterization and properties of pre beta-HDL particles formed by ABCA1-mediated cellular lipid efflux to apoA-I. *J Lipid Res*. 2008;49:1006–1014. doi: 10.1194/jlr.M700506-JLR200
- Krimbou L, Hajj Hassan H, Blain S, Rashid S, Denis M, Marcil M, Genest J. Biogenesis and speciation of nascent apoA-I-containing particles in various cell lines. *J Lipid Res*. 2005;46:1668–1677. doi: 10.1194/jlr.M500038-JLR200

23. Hayashi M, Abe-Dohmae S, Okazaki M, Ueda K, Yokoyama S. Heterogeneity of high density lipoprotein generated by ABCA1 and ABCA7. *J Lipid Res.* 2005;46:1703–1711. doi: 10.1194/jlr.M500092-JLR200
24. Liu L, Bortnick AE, Nickel M, Dhanasekaran P, Subbaiah PV, Lund-Katz S, Rothblat GH, Phillips MC. Effects of apolipoprotein A-I on ATP-binding cassette transporter A1-mediated efflux of macrophage phospholipid and cholesterol: formation of nascent high density lipoprotein particles. *J Biol Chem.* 2003;278:42976–42984. doi: 10.1074/jbc.M308420200
25. Forte TM, Goth-Goldstein R, Nordhausen RW, McCall MR. Apolipoprotein A-I-cell membrane interaction: extracellular assembly of heterogeneous nascent HDL particles. *J Lipid Res.* 1993;34:317–324.
26. Herzog E, Pragst I, Waelchli M, Gille A, Schenk S, Mueller-Cohrs J, Diditchenko S, Zanoni P, Cuchel M, Seubert A, et al. Reconstituted high-density lipoprotein can elevate plasma alanine aminotransferase by transient depletion of hepatic cholesterol: role of the phospholipid component. *J Appl Toxicol.* 2016;36:1038–1047. doi: 10.1002/jat.3264
27. Matz CE, Jonas A. Micellar complexes of human apolipoprotein A-I with phosphatidylcholines and cholesterol prepared from cholate-lipid dispersions. *J Biol Chem.* 1982;257:4535–4540.
28. Lerch PG, Förtsch V, Hodler G, Bolli R. Production and characterization of a reconstituted high density lipoprotein for therapeutic applications. *Vox Sang.* 1996;71:155–164. doi: 10.1046/j.1423-0410.1996.71.30155.x
29. Barter PJ, Chang LB, Newnam HH, Rye KA, Rajaram OV. The interaction of cholesteryl ester transfer protein and unesterified fatty acids promotes a reduction in the particle size of high-density lipoproteins. *Biochim Biophys Acta.* 1990;1045:81–89. doi: 10.1016/0005-2760(90)90206-d
30. Van Sickle WA, Wilcox HG, Nasjletti A. HDL-induced cardiac prostacyclin synthesis: relative contribution of HDL apoprotein and lipid. *Biochem Biophys Res Commun.* 1986;139:416–423. doi: 10.1016/s0006-291x(86)80007-9
31. Sankaranarayanan S, Kellner-Weibel G, de la Llera-Moya M, Phillips MC, Asztalos BF, Bittman R, Rothblat GH. A sensitive assay for ABCA1-mediated cholesterol efflux using BODIPY-cholesterol. *J Lipid Res.* 2011;52:2332–2340. doi: 10.1194/jlr.D018051
32. Wyatt PJ. Light scattering and the absolute characterization of macromolecules. *Analytica Chimica Acta.* 1993;272:1–40.
33. Mashaghi A, Swann M, Popplewell J, Textor M, Reimhult E. Optical anisotropy of supported lipid structures probed by waveguide spectroscopy and its application to study of supported lipid bilayer formation kinetics. *Anal Chem.* 2008;80:3666–3676. doi: 10.1021/ac800027s
34. Tumolo T, Angnes L, Baptista MS. Determination of the refractive index increment (dn/dc) of molecule and macromolecule solutions by surface plasmon resonance. *Anal Biochem.* 2004;333:273–279. doi: 10.1016/j.ab.2004.06.010
35. Ronsein GE, Vaisar T. Inflammation, remodeling, and other factors affecting HDL cholesterol efflux. *Curr Opin Lipidol.* 2017;28:52–59. doi: 10.1097/MOL.0000000000000382
36. Bailey D, Ruel I, Hafiane A, Cochrane H, Iatan I, Jauhiainen M, Ehnholm C, Krimbou L, Genest J. Analysis of lipid transfer activity between model nascent HDL particles and plasma lipoproteins: implications for current concepts of nascent HDL maturation and genesis. *J Lipid Res.* 2010;51:785–797. doi: 10.1194/jlr.M001875
37. Wang N, Tall AR. Regulation and mechanisms of ATP-binding cassette transporter A1-mediated cellular cholesterol efflux. *Arterioscler Thromb Vasc Biol.* 2003;23:1178–1184. doi: 10.1161/01.ATV.0000075912.83860.26
38. Mulya A, Lee JY, Gebre AK, Thomas MJ, Colvin PL, Parks JS. Minimal lipidation of pre-beta HDL by ABCA1 results in reduced ability to interact with ABCA1. *Arterioscler Thromb Vasc Biol.* 2007;27:1828–1836. doi: 10.1161/ATVBAHA.107.142455
39. Fielding CJ, Fielding PE. Molecular physiology of reverse cholesterol transport. *J Lipid Res.* 1995;36:211–228.
40. Nanjee MN, Brinton EA. Very small apolipoprotein A-I-containing particles from human plasma: isolation and quantification by high-performance size-exclusion chromatography. *Clin Chem.* 2000;46:207–223.
41. Miller NE, Olszewski WL, Hattori H, Miller IP, Kujiraoka T, Oka T, Iwasaki T, Nanjee MN. Lipoprotein remodeling generates lipid-poor apolipoprotein A-I particles in human interstitial fluid. *Am J Physiol Endocrinol Metab.* 2013;304:E321–E328. doi: 10.1152/ajpendo.00324.2012
42. Nanjee MN, Cooke CJ, Olszewski WL, Miller NE. Concentrations of electrophoretic and size subclasses of apolipoprotein A-I-containing particles in human peripheral lymph. *Arterioscler Thromb Vasc Biol.* 2000;20:2148–2155. doi: 10.1161/01.atv.20.9.2148
43. Nguyen D, Nickel M, Mizuguchi C, Saito H, Lund-Katz S, Phillips MC. Interactions of apolipoprotein A-I with high-density lipoprotein particles. *Biochemistry.* 2013;52:1963–1972. doi: 10.1021/bi400032y
44. Ahmed SN, Brown DA, London E. On the origin of sphingolipid/cholesterol-rich detergent-insoluble cell membranes: physiological concentrations of cholesterol and sphingolipid induce formation of a detergent-insoluble, liquid-ordered lipid phase in model membranes. *Biochemistry.* 1997;36:10944–10953. doi: 10.1021/bi971167g
45. Mulya A, Lee JY, Gebre AK, Boudyguina EY, Chung SK, Smith TL, Colvin PL, Jiang XC, Parks JS. Initial interaction of apoA-I with ABCA1 impacts *in vivo* metabolic fate of nascent HDL. *J Lipid Res.* 2008;49:2390–2401. doi: 10.1194/jlr.M800241-JLR200
46. Sloop CH, Dory L, Roheim PS. Interstitial fluid lipoproteins. *J Lipid Res.* 1987;28:225–237.
47. Parini P, Johansson L, Bröijersén A, Angelin B, Rudling M. Lipoprotein profiles in plasma and interstitial fluid analyzed with an automated gel-filtration system. *Eur J Clin Invest.* 2006;36:98–104. doi: 10.1111/j.1365-2362.2006.01597.x
48. Gao X, Jayaraman S, Gursky O. Mild oxidation promotes and advanced oxidation impairs remodeling of human high-density lipoprotein *in vitro*. *J Mol Biol.* 2008;376:997–1007. doi: 10.1016/j.jmb.2007.12.030
49. Shao B, Oda MN, Bergt C, Fu X, Green PS, Brot N, Oram JF, Heinecke JW. Myeloperoxidase impairs ABCA1-dependent cholesterol efflux through methionine oxidation and site-specific tyrosine chlorination of apolipoprotein A-I. *J Biol Chem.* 2006;281:9001–9004. doi: 10.1074/jbc.C600011200
50. Hewing B, Parathath S, Barrett T, Chung WK, Astudillo YM, Hamada T, Ramkhalawon B, Tallant TC, Yusufshaq MS, Didonato JA, et al. Effects of native and myeloperoxidase-modified apolipoprotein a-I on reverse cholesterol transport and atherosclerosis in mice. *Arterioscler Thromb Vasc Biol.* 2014;34:779–789. doi: 10.1161/ATVBAHA.113.303044
51. Cimmino G, Ibanez B, Vilahur G, Speidl WS, Fuster V, Badimon L, Badimon JJ. Up-regulation of reverse cholesterol transport key players and rescue from global inflammation by ApoA-I(Milano). *J Cell Mol Med.* 2009;13(9B):3226–3235. doi: 10.1111/j.1582-4934.2008.00614.x
52. Murphy AJ, Funt S, Gorman D, Tall AR, Wang N. Pegylation of high-density lipoprotein decreases plasma clearance and enhances antiatherogenic activity. *Circ Res.* 2013;113:e1–e9. doi: 10.1161/CIRCRESAHA.113.301112
53. Shaw JA, Bobik A, Murphy A, Kanellakis P, Blomberg P, Mukhamedova N, Woollard K, Lyon S, Sviridov D, Dart AM. Infusion of reconstituted high-density lipoprotein leads to acute changes in human atherosclerotic plaque. *Circ Res.* 2008;103:1084–1091. doi: 10.1161/CIRCRESAHA.108.182063
54. ClinicalTrials.gov. Study to Investigate CSL112 in Subjects With Acute Coronary Syndrome (AEGIS-II). Available at: <https://clinicaltrials.gov/ct2/show/NCT03473223>. Accessed May 11, 2019.
55. Nicholls SJ, Andrews J, Kastelein JJP, Merkely B, Nissen SE, Ray KK, Schwartz GG, Worthley SG, Keyserling C, Dasseux JL, et al. Effect of serial infusions of CER-001, a pre-β high-density lipoprotein mimetic, on coronary atherosclerosis in patients following acute coronary syndromes in the CER-001 Atherosclerosis Regression Acute Coronary Syndrome Trial: a Randomized Clinical Trial. *JAMA Cardiol.* 2018;3:815–822. doi: 10.1001/jamacardio.2018.2121
56. Nicholls SJ, Puri R, Ballantyne CM, Jukema JW, Kastelein JJP, Koenig W, Wright RS, Kallend D, Wijngaard P, Borgman M, et al. Effect of infusion of high-density lipoprotein mimetic containing recombinant apolipoprotein A-I milano on coronary disease in patients with an acute coronary syndrome in the MILANO-PILOT Trial: a Randomized Clinical Trial. *JAMA Cardiol.* 2018;3:806–814. doi: 10.1001/jamacardio.2018.2112
57. Rader DJ. Apolipoprotein A-I infusion therapies for coronary disease: two outs in the ninth inning and swinging for the fences. *JAMA Cardiol.* 2018;3:799–801. doi: 10.1001/jamacardio.2018.2168
58. Bolin DJ, Jonas A. Sphingomyelin inhibits the lecithin-cholesterol acyltransferase reaction with reconstituted high density lipoproteins by decreasing enzyme binding. *J Biol Chem.* 1996;271:19152–19158. doi: 10.1074/jbc.271.32.19152
59. Calabresi L, Franceschini G, Burkybile A, Jonas A. Activation of lecithin cholesterol acyltransferase by a disulfide-linked apolipoprotein A-I dimer. *Biochem Biophys Res Commun.* 1997;232:345–349. doi: 10.1006/bbrc.1997.6286
60. Roma P, Gregg RE, Meng MS, Ronan R, Zech LA, Franceschini G, Sirtori CR, Brewer HB Jr. *In vivo* metabolism of a mutant form of apolipoprotein A-I, apo A-IMilano, associated with familial hypoalphalipoproteinemia. *J Clin Invest.* 1993;91:1445–1452. doi: 10.1172/JCI116349
61. Kempen HJ, Schranz DB, Asztalos BF, Otvos J, Jeyarajah E, Drazul-Schrader D, Collins HL, Adelman SJ, Wijngaard PL. Incubation of MDCO-216 (ApoA-IMilano/POPC) with human serum potentiates ABCA1-mediated cholesterol efflux capacity, generates new prebeta-1 HDL, and causes an increase in HDL size. *J Lipids.* 2014;2014:923903. doi: 10.1155/2014/923903